Modelling spatial and temporal leaf temperature dynamics a focus on the leaf boundary layer

M. Saudreau, Boris B. Adam, Amelie Ezanic, Sylvain Pincebourde

M. Saudreau, Boris B. Adam, Amelie Ezanic, Sylvain Pincebourde. Modelling spatial and temporal leaf temperature dynamics a focus on the leaf boundary layer. 7. International Conference on Functional-Structural Plant Models, FSPM., Jun 2013, Sariselka, Finland. pp.146-148. hal-02744825

HAL Id: hal-02744825
https://hal.inrae.fr/hal-02744825v1

Proceedings of the 7th International Conference on Functional-Structural Plant Models, Saariselkä, Finland, 9 - 14 June 2013. Eds. Risto Sievänen, Eero Nikinmaa, Christophe Godin, Anna Lintunen & Pekka Nygren. http://www.metal.fi/fspm2013/proceedings. ISBN 978-951-651-408-9.

Modelling Spatial and Temporal Leaf Temperature Dynamics
A focus on the leaf boundary layer

Marc Saudreau [1,2,*], **Boris Adam** [1,2], **Amélie Ezanic** [3] **and Sylvain Pincebourde** [3]
[1]*INRA, UMR547 PIAF, F-63100 Clermont-Ferrand, France,* [2]*UBP, UMR547 PIAF, F- 63000 Aubière, France,* [3]*IRBI, IRBI UMR CNRS 7261, Université de Tours, Tours, France*
**correspondence:* marc.saudreau@clermont.inra.fr

Highlights: A 3D leaf temperature model is proposed to estimate dynamics of temperature gradients at leaf surface. The 3D leaf shape, the leaf physiology, and the microclimate are accounted for. Computational Fluid Dynamics was used to simulate realistic spatial evolution of the sensible heat flux at the leaf surface.

Keywords: 3D Leaf Model, Heat balance, Nusselt Number, Free Convection, Boundary Layer

INTRODUCTION

Leaf temperature is an important factor involved in many biological processes such as leaf transpiration and photosynthesis (Gates 1968), leaf – pathogen interactions (Bernard et al. 2013) or insect development rates (Beck 1983). Within a plant canopy, leaves can exhibit a wide variety of temperature dynamics (frequency, amplitude, spatial gradients) related to the leaf position within the canopy (sunlit vs shaded leaf), the leaf shape and orientation (small vs large, downward vs upward), the leaf physiology (stomatal regulation), and the variability in microclimatic conditions (wind, light, air temperature and air relative humidity). Such variability in leaf temperature dynamics result from changes in heat energy exchanges between the leaf and its local environment. The underlying physics is well known and the temperature dynamics can be inferred by solving a heat balance equation where microclimate and leaf physiology are taken into account through radiation (R), convection (C), evapotranspiration (λE) and diffusion (G) terms: $R + C + \lambda E + G = 0$ (Monteith and Unsworth 1990). Among these terms, the convective term (C) is definitively the more difficult to estimate because it describes the heat transfer process due to the leaf boundary layer.

Many leaf energy models have been developped so far and have been integrated in crop and plant canopy models (Sinoquet et al. 2001; Brisson et al. 2003) but they only simulate the dynamics of the spatially average leaf temperature. Our aim was to build up a flexible and fast 3D leaf temperature model to predict main trends of spatial temperature patterns dynamics at leaf surface. Both leaf geometry, leaf physiology and microclimate were accounted for (Fig. 1). Based on theoretical and Computational Fluid Dynamics (CFD) results, forced and free laminar boundary layers were implemented for the convective term. The free convective boundary layer implementation and the 3D model are presented and discussed.

THE 3D LEAF TEMPERATURE MODEL

Among the different terms of the heat balance equation presented above, the diffusion term and the leaf thickness are neglected ($G \approx 0$), based upon values of the leaf thickness (~10^{-4} m) and the leaf thermal conductivity (0.4 $W.m^{-1}.K^{-1}$ (Vogel 1983)), and the time step used (from 30 minutes to one hour). Thus, the leaf volume is assumed to be zero and the surface is decomposed into n triangles.

On each triangle, the heat balance equation is solved following Monteith and Unsworth (1990): $R + C + \lambda E = 0$. The radiation heat flux is split into a direct and a diffuse component, and PAR and NIR wavebands are considered. The convective and evapotranspirative heat fluxes are modelled using classical relationships (Monteith and Unsworth 1990). The Jarvis model is used for the leaf stomatal conductance (Damour et al. 2010).

The entire leaf temperature model is written in Python. Numerical integrations and the iterative procedure used to solve the heat balance equation are based upon numpy and scipy libraries (Jones et al. 2001).

Both theoretical (plates) and real (3D scanned apple leaves) surfaces were used to assess the model and to perform temperature computations.

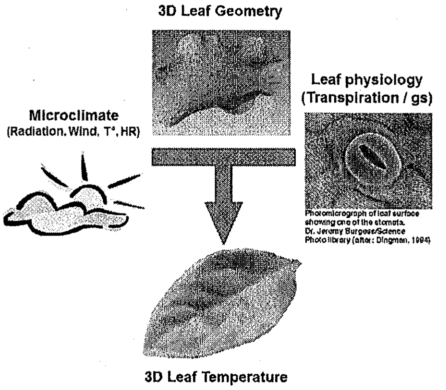

Fig. 1. Schematic view of the main features of the 3D leaf model

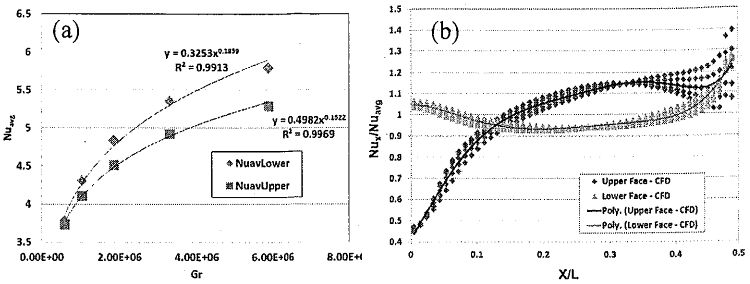

Fig. 2. Free convection – CFD results: (a) Average Nusselt number function of the buoyancy force intensity: $Nu_{avg} = 1/L \int_L Nu_x dx$, and (b) Local Nusselt number Nu_x/Nu_{avg} along the main axis for several Grashof numbers ($X/L = 0$ corresponds to the plate center and $X/L = 0.5$ to the edge of the plate).

THE BOUNDARY LAYER

Loss of energy by the leaf boundary layer is highly dependent on the main force driving the flow (Schuepp 1993). For a leaf, two forces could induce a movement of the air at its surface: the inertial force due to the main outer flow (i.e. the wind speed *U*), and the buoyancy force due to temperature gradient between the leaf surface (*Tleaf*) and the air (*Tair*). If the flow imposed by the external wind is weaker than the flow induced by the temperature difference between the leaf and the surrounding air, the convection is defined as "free". On the contrary if the boundary layer is driven by the external wind flow the convection is defined as "forced". The flow pattern and thus the heat exchange coefficient pattern dramatically change from a "free" to a "forced" convection The convective heat transfer per unit of surface is defined by $h(Tleaf - Tair)$ where h is the heat transfer coefficient ($W.m^{-2}.K^{-1}$). For convenience of scaling, the Nusselt number (*Nu*) defined as $Nu = \frac{h.L}{k}$, where L is a characteristic length scale (m), and k is the thermal conductivity of air ($W.m^{-1}.K^{-1}$), is used instead of h (Monteith and Unsworth 1990).

The intensity of free and forced convection can be estimated with the Grashof number (the ratio of buoyancy force to viscous force - $Gr=\beta gL^3(T_{leaf}-T_{air})/\nu^2$) and the Reynolds number (the ratio of inertial force to viscous force - $Re=UL/\nu$) (Monteith and Unsworth 1990) where β (K^{-1}) is the thermal expansion coefficient of the air, g ($m.s^{-2}$) is the acceleration of the gravity, and ν ($m^2.s^{-1}$) the kinematic viscosity of the air. Theoretical and experimental results have shown that the Nusselt numbers for free and forced convections are proportional to Gr^a and Re^b respectively (Schuepp 1993). The use of CFD (Comsol Multiphysics v4.3a) enables us to estimate the exponent coefficients a and b for a wide variety of driving force intensity and surface geometry.

Based on simple geomerical considerations (distance from the leaf leading edge according to the wind direction, distance from the leaf edge, main surface inclination angle) and estimates of Nusselt numbers from CFD, both kind of convection type were implemented in the 3D Leaf model.

RESULTS AND DISCUSSION

Figure 2a shows the effect of Grashof number on average Nusselt numbers for a horizontal thin plate. For both faces the Nusselt number exibits an exponential relationship with the Grashof number: $Nu \sim m.Gr^a$ with $a \approx 0.186$,$m \approx 0.325$ for the lower face, and $a \approx 0.152$, $m \approx 0.498$ for the lower faces. These values are in agreement with the study of Wei et al. (2002) who performed numerical simulations of the natural convection heat transfer for an uniformly heated plate with metallic physical properties: $a \approx 0.2$, $m \approx 0.317$ and $a \approx 0.16$, $m \approx 0.675$ for the lower and upper faces respectively. Some heat transfer observations from uniformly heated metallic leaf models are available from early studies of Knoerr and Gay (1965) and Dixon and Grace (1983). They reported values of a between 0.1 and 0.2.

For several Grashof numbers i.e. free convection intensities, the ratio between the local Nusselt number Nu_x and the average Nusselt number Nu_{avg} (see figure 2a) along the main axis of the plate is plotted in figure 2b. For the range of Grashof numbers investigated, the ratio Nu_x/Nu_{avg} do not change with Gr except at the edge of the upper face. The Nusselt number presents different patterns between faces with a quasi flat curve at the lower face except at the edge, and with increasing values from the plate center to the edge for the upper face. The ratio Nu_x/Nu_{avg} can be fitted with 5th and 6th order polynomial functions with R^2 coefficient up to 0.94 for lower and upper faces respectively.

The above CFD results show that some simple and robust relationships of heat transfer coefficients can be found for a free laminar convective boundary layer. Of course leaf boundary layers could exhibit local and sudden patterns for high inclination angle of the surface or when high wind velocity promotes the transition to turbulence of the leaf boundary layer, and the creation of large energetic structures in the trailing edge of the leaf. Such situations cannot be handled with the above relationships.

Above relationships of local and average heat transfer coefficients Nu_x *(x/L)* and Nu_{avg}*(Gr)* of free laminar convective boundary layer for both lower face and upper face were implemented in the 3D leaf model (figure 3a). Based upon such results and when all features of the 3D leaf model are used together, leaf temperature heterogeneity can be revealed (Figure 3b). In the future, a sensitivity analysis of the main parameters of the model and a model assessment based on IR infra-red camera measurements will be performed.

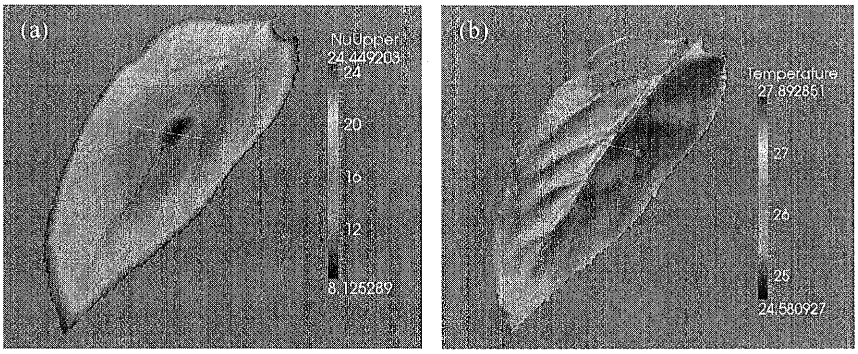

Fig. 3. Illustrations of (i) the Nusselt number implementation for a free convection for an horizontal 3D leaf model (a), and of (ii) a simulated temperature pattern according to given microclimate characteristics (b).

LITERATURE CITED

Beck SD. 1983. Insect Thermoperiodism *Annual Review of Entomology* **28**:91-108

Brisson NC, Gary et al. 2003. An overview of the crop model stics. *European Journal of Agronomy* **18(3–4)**: 309-332.

Bernard F, Sache I, Suffert F and Chelle M. 2013. The development of a foliar fungal pathogen does react to leaf temperature! *New Phytologist*, **198**: 232–240

Damour G, Simonneau T, Cochard H, Urban L. 2010. An overview of models of stomatal conductance at the leaf level, *Plant Cell and Environment*, **33(9):**1419-38

Dixon M and Grace J. 1983. Natural convection from leaves at realistic Grashof numbers. *Plant, Cell & Environment* **6(8)**: 665-670.

Gates D. M. 1968. "Transpiration and Leaf Temperature." *Annual Review of Plant Physiology* **19(1)**: 211-238

Jones E, Oliphant T., Peterson P et al. 2001. SciPy: Open Source Scientific Tools for Python, http://www.scipy.org

Knoerr KR and Gay LW. 1965. Tree Leaf Energy Balance, *Ecology* **46**: 17-24

Monteith J and Unsworth MH. 1990. *Principles of environmental physics*, 2nd edn. Edward Arnold, London, pp. 291.

Schuepp PH. 1993. Tansley review no. 59: Leaf boundary-layers. *New Phytologist* **125(3):** 477-507.

Sinoquet H, Le Roux X, Adam B, Ameglio T, Daudet FA. 2001. RATP: a model for simulating the spatial distribution of radiation absorption, transpiration and photosynthesis within canopies: application to an isolated tree crown. *Plant, Cell and Environment* **24:** 395–406.

Vogel S. 1983. The lateral thermal conductivity of leaves, *Canadian. Journal of Botany*, **62**:741-744

Wei JJ, Yu B, et al. 2002. Numerical study of simultaneous natural convection heat transfer from both surfaces of a uniformly heated thin plate with arbitrary inclination. *Heat and Mass Transfer* **38(4):** 309-317.

ACKWNOLEDGEMENT

This work was funded by the French National Research Agency project MicroCliMite No ANR-10-BLAN-01706-02